Organic & Biomolecular Chemistry

Dynamic Article Links

Cite this: *Org. Biomol. Chem.*, 2011, **9**, 8079

www.rsc.org/obc

PAPER

Origins of the diastereoselectivity in hydrogen bonding directed Diels–Alder reactions of chiral dienes with achiral dienophiles: a computational study†

Sesil Agopcan, Nihan Çelebi-Ölçüm,‡ Melek Nihan Üçışık,§ Amitav Sanyal and Viktorya Aviyente*

Received 28th July 2011, Accepted 31st August 2011
DOI: 10.1039/c1ob06285a

In this study, the origins of diastereoselectivity in the hydrogen bonding assisted Diels–Alder reactions of chiral dienes with achiral dienophiles have been investigated with density functional methods. The distortion/interaction model has been applied to shed light on the origins of selectivity. C9-Substituted chiral anthracene templates (R = $(CH_3)(OCH_3)(H)$, R = $(CH_3)(OH)(H)$, R = $(CH_3)(CH_2CH_3)(H)$ and R = $(-CH_2-C(CH_3)(OCH_3)(H))$ are used to rationalize the role of a stereogenic center and H-bonding on the product distribution ratio. Even though hydrogen bonding increases the reactivity of the diene, the stereoselectivity is reduced because of the hydrogen bonding capacity of both diastereomeric transition states. The interaction energies of the studied anthracene templates with *N*-methyl maleimide at the transition state correlate linearly with an increase in reactivity. The selectivity is determined by both favorable distortion and interaction energies. The π-facial selectivity induced by the presence of a chiral auxiliary in 1-substituted 1,3-pentadienes (R1 = $(CH_3)(OCH_3)(H)$ and R1 = $(CH_3)(OH)(H)$) has also been modeled in order to rationalize the role of the stereogenic center and H-bonding on the stereoselectivity of an aliphatic diene. In both parts, the product distribution ratios calculated from Boltzmann distributions based on Gibbs free energies are in reasonable agreement with the experimental results. Finally the role of OH-substituted five-membered pyrrolidine on C9 of anthracene is investigated since the successful usage of the conformationally rigid pyrrolidines in asymmetric synthesis is well known. Overall, both in the acyclic system and in anthracene, the facilitation due to H-bonding is reflected in the interaction energies: the higher the difference in interaction energies in the transition structures of the two diastereomers, the more selective the H-bonding assisted Diels–Alder reaction is.

Introduction

The asymmetric Diels–Alder reaction is one of the most powerful and widely utilized processes to access enantiopure six-membered cycles. An exciting advance in asymmetric Diels–Alder chemistry is the use of chiral dienes as stereodirecting elements to yield cycloadducts with high enantiomeric and diastereomeric excesses.[1–6] The utilization of chiral dienes opens up the possibility of stereoselectively functionalizing achiral dienophiles by means of a Diels–Alder/retro-Diels–Alder sequence.[2–4] The Diels–Alder/retro-Diels–Alder strategy involves a binding–transforming–releasing sequence, which can be regarded as a basic mimic of enzymes, nature's complex homochiral templates for stereoselective transformations. The sequence (Scheme 1) starts with the cycloaddition of the achiral dienophile with the chiral diene template to give a diastereomerically pure cycloadduct. The stereocenters on the cycloadduct allow enantioselective functionalization of the dienophile subunit, which finally is released in the cycloreversion step.

The Diels–Alder/retro-Diels–Alder methodology has received substantial interest and has been successfully employed towards the synthesis of many complex bioactive molecules in their enantiomerically pure forms.[2–4] Cyclopentadiene derivatives have found extensive use as chiral diene templates for stereoselective transformations of various dienophiles.[2] More recently, chiral 9-substituted anthracene templates have been successfully employed for the preparation of α,β-butenolides and α,β-unsaturated lactams with high enantiomeric excess.[4,5] The selection of the appropriate diene template is of significant importance, as all the additions to the 4π system should take place with excellent enantio-, diastereo- and regioselectivity. The stereochemical outcome of the sequence is vastly determined by the levels of selectivity obtained in the initial Diels–Alder cycloaddition step. An understanding of the key factors that determine the reactivity and selectivity of asymmetric cycloadditions of chiral dienes with various

Department of Chemistry, Boğaziçi University, Bebek, Istanbul, 34342, Turkey. E-mail: aviye@boun.edu.tr

† Electronic supplementary information (ESI) available: Coordinates and 3D structures of reactants, transition states and products. See DOI: 10.1039/c1ob06285a

‡ Current address: Department of Chemistry and Biochemistry, University of California, Los Angeles, California 90095-1569, USA.

§ Current address: Department of Chemistry, Quantum Theory Project, University of Florida, Gainesville, Florida 32611-8435, USA.

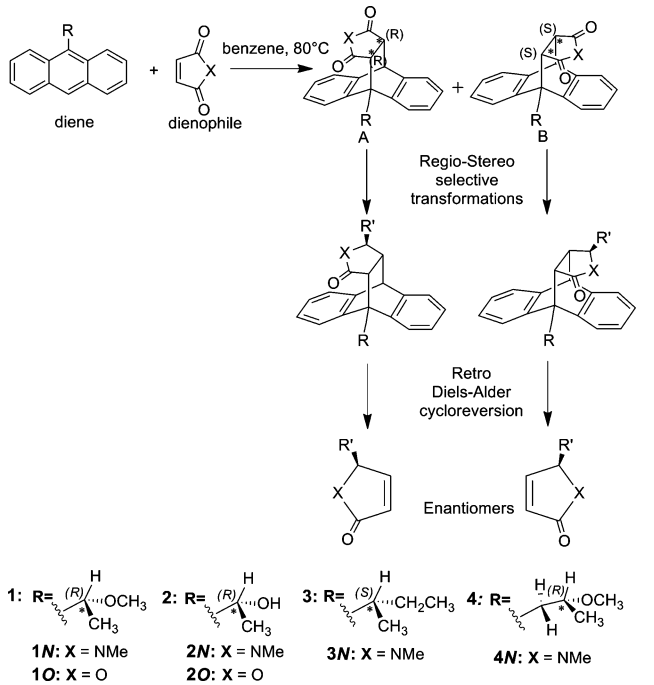

Scheme 1 Stereoselective functionalization of the dienophile using a chiral anthracene template.[6]

dienophiles is particularly important to increase the efficiency of similar transformations that find extensive use in the synthesis of complex bioactive molecules.

Due to the usefulness and wide application area of asymmetric Diels–Alder chemistry, a lot of effort has been devoted to exploring the origins of selectivity in a variety of asymmetric Diels–Alder reactions. Among the numerous studies of Houk on Diels–Alder reactions,[7] one can cite stereoselective cycloadditions that probe substituent effects in aryl–aryl sandwich complexes,[7a] the Diels–Alder reaction of terminal-substituted dienes and dienophiles yielding *exo* selectivity,[7b] the Diels–Alder reactions of cyclopentadiene and 9,10-dimethylanthracene with cyanoalkenes,[7c] the cycloadditions of 1-methoxy-4-trimethylsiloxy dienes with acrylonitrile[7d] and the predictions of the stereoselective antibody catalysis of several different types of Diels–Alder reactions.[7e–7g] Houk and co-workers. have recently described the computational design and experimental characterization of enzymes catalyzing a bimolecular Diels–Alder reaction with high stereoselectivity and substrate specificity.[7h] A computational comparison of the Diels–Alder reaction of maleimide and anthracene in water and the active site of the ribozyme Diels–Alderase is reported by Bruice and Zhang.[8] Beside the catalytic effect of an hydrogen bond between the diene and dienophile in the transition state,[9] the importance of hydrogen bonding in controlling the stereochemical outcome of the Diels–Alder reactions has also been proposed by various groups.[10] Meijer and co-workers have recently studied the diastereoselective cycloadditions and transformations of *N*-alkyl and *N*-aryl maleimides with chiral 9-anthrylethanol derivatives both experimentally and computationally.[11] We now show that the effect of the stereodirecting group on the interaction energy between the diene and the dienophile at the transition state is responsible both for the rate enhancement and the stereochemical outcome of the reaction.

We have recently studied the Diels–Alder reactions of C9-substituted chiral anthracenes with maleic anhydride using DFT and identified the key interactions in the transition state.[6] Here, we use DFT calculations and the distortion–interaction model[12] to explain the origins of the chiral induction in Diels–Alder reactions of chiral dienes with achiral dienophiles. In the first part, we describe the cycloadditions of C9-substituted anthracenes and maleate derivatives and explain the stereochemical nature of the Diels–Alder reaction, the importance of the location of the stereocenter as well as the effect of hydrogen bonding on the stereoselectivity. In the second part, the mechanistic aspect of the π-facial selectivity is compared to the stereoselectivity induced by a C9-chiral auxiliary substituted anthracene. In part three, the common features of both parts are highlighted by making use of the asynchronicity in the transition structures, the kinetic barriers and the thermodynamic character of the reactions. Finally part four includes the investigation of the role of a rigid five-membered chiral auxiliary substituent on C9 of anthracene inspired by Rawal and co-workers,[1] in order to inquire whether the diastereoselectivity of the reaction increases by hydrogen bonding in the reaction of (2*R*,5*R*)-1-(anthracen-9-yl)-5-methoxypyrrolidin-2-ol and maleic anhydride.

Computational methodology

Computational studies on similar reactions in the last decade have been considered in order to assess the methodology used in this study. The pseudo-intramolecular Diels–Alder reaction between a 2-substituted furan and *N*-maleimide has been analyzed using the B3LYP functional with the 6-31G(d,p) basis set.[13a] In the study of halo substituent effects on intramolecular cycloadditions involving furanyl amides B3LYP/6-31G(d) is claimed to yield a trend similar to the highly accurate CBS-QB3 level of theory.[13b] Nevertheless, the same group has used CBS-QB3 computations to explore the halogen effect on the reactivity and reversibility on Diels–Alder cycloadditions involving furan.[13c] B3LYP/6-31G* has also been employed in the Diels–Alder reaction between acetylenedicarboxylic acid and 1,3-bis(2-furyl)propane.[14]

Based on the widespread usage of B3LYP[15] for Diels–Alder reactions, on its cost-effective character, and on the large number of conformations explored in this study, optimizations have been carried out with B3LYP/6-31+G(d) in Gaussian 03.[16] A conformational analysis of the dienes, of their transition structures with **NMM** and **MA** and of their adducts has been carried out with PM3 and all the geometries corresponding to local minima (3^n where n is the number of single bonds) have been reoptimized with B3LYP/6-31+G(d); the conformations with this method are displayed in Figures S1–S4.† A frequency analysis has been performed in order to identify the nature of the stationary points and also to have zero point energies and thermal corrections. Transition states were identified by the presence of a single imaginary vibrational frequency. IRC calculations with B3LYP/6-31+G(d) have been carried out in order to justify the nature of the reactants and products.[17]

The stationary points located with B3LYP/6-31+G(d) were further optimized with BMK/6-31+G(d) in Gaussian 09[18] in order to confirm the geometries and energetics of the systems of interest. The BMK (Boese–Martin for kinetics) functional has an excellent performance for barrier heights. BMK has a

combined penalty function (involving about 500 systems) in which barrier heights were assigned large weights.[19] Energetics have also been evaluated with M06-2X/6-31+G(d)[20] utilizing the B3LYP/6-31+G(d) geometries. The M06-2X functional is a high nonlocality functional with double the amount of nonlocal exchange (2X), and it is parametrized only for nonmetals.[20] Based on Gibbs free energies of activation at the B3LYP/6-31+G(d), the BMK/6-31+G(d) and M06-2X/6-31+G(d)//B3LYP/6-31+G(d) levels, the population of the diastereomers has been evaluated by using the Boltzmann distribution at 80 °C for reactions of anthracene derivatives and at 25 °C for reactions of 1-substituted-1,3-pentadienes. Stereoselectivities predicted at the BMK/6-31+G(d) and M06-2X/6-31+G(d)//B3LYP/6-31+G(d) levels agree well with the B3LYP/6-31G(d) results (Table S1, Table S2†). We discuss the B3LYP/6-31G(d) results in the text; the BMK/6-31+G(d) and M06-2X/6-31+G(d)//B3LYP/6-31+G(d) results are displayed in the supporting information.

Single point solvent calculations were carried out with the Polarizable Continuum Model (PCM) using the integral equation formalism variant (IEFPCM) and the bondi cavity model in Gaussian 03.[21a,b] Benzene is used as a solvent to reproduce the experimental conditions (ε = 2.2706). We used the ideal gas approximation and assumed T = 298.15 K and 1 atm (gas phase) or 1 M concentration (solution). The computation of free energies of activation in solution was done according to typical procedures based on thermodynamic cycles. Accordingly, solvation free energies include a correction to account for a change in reference state (This change is RTln(24.5) and 1.89 kcal mol^{-1} at 298.15 K).[21c,d]

The distortion–interaction model is used to analyze the energy barriers: this method is a fragment-based approach used to understand chemical reactions and the associated barriers.[12f] The starting point is the two separate reactants, which approach from infinity and begin to interact and deform each other. The distortion–interaction model partitions the activation energy ($\Delta E_0^{\ddagger}$) into distortion energy ($\Delta E_{dist}^{\ddagger}$), and interaction energy ($\Delta E_{int}^{\ddagger}$) between distorted fragments, where the former is associated with the strain caused by deforming the individual reactants, and the latter is the favorable interaction between the deformed reactants.[12]

$$\Delta E_0^{\ddagger} = \Delta E_{dist}^{\ddagger} + \Delta E_{int}^{\ddagger}$$

All energies are reported in kcal mol^{-1} and distances in angstroms.

Results and discussion

1. Stereogenic center and hydrogen bonding effects on the Diels–Alder reactions of anthracene derivatives

The diastereoselective addition of an alkene occurs across the 9 and 10 positions of the anthracene moiety, the selectivity of which is controlled by the stereogenic center pendant from the anthracene. The effect of the dienophile on the selectivity of the reaction is monitored experimentally by altering the dienophile from *N*-methylmaleimide (**NMM**) to maleic anhydride (**MA**) (Scheme 1). The role of H-bonding can be elucidated by comparing reactions **1** (R = (CH_3)(OCH_3)(H)) and **2** (R = (CH_3)(OH)(H)). In reaction **3** (R = (CH_3)(CH_2CH_3)(H)) the stereogenic center bears alkyl groups only. In reaction **4** (R = (-CH_2-C(CH_3)(OCH_3)(H)) the stereogenic center is moved one carbon away from C9 and is not directly attached to anthracene.

Reaction of 1 with NMM and MA. The reaction of the chiral compound **1** with **NMM** yields diastereomer **A** preferentially *via* **TS1*N*-A** (Fig. 1) where the oxygen (–0.419) of **NMM** and the hydrogen of the methoxy group (0.234) favorably interact with each other (2.73 Å) and stabilize this structure: **TS1*N*-B** is 3.3 kcal mol^{-1} higher than **TS1*N*-A**. Even though the O (–0.418) ··· H (0.263) stabilizing interaction is stronger (2.50 Å) in **TS1*N*-B** than it is in **TS1*N*-A**, **TS1*N*-A** is earlier, more synchronous and less distorted than **TS1*N*-B**. In the case of **TS1*O*-A**, the carbonyl oxygen (–0.372) on **MA** interacts with the H on the methoxy group (0.230) of anthracene (2.82 Å) allowing a sterically less hindered approach of the dienophile to the diene (Fig. 2). **TS1*O*-B** is less synchronous and 3.6 kcal mol^{-1} higher in energy than **TS1*O*-A**. The latter has two stabilizing interactions between the carbonyl oxygen of **MA** (–0.372) and the H of –OCH_3 (0.230) and also between the oxygen of the methoxy group (–0.166) and the hydrogen of the **MA** (0.275). In **TS1*O*-B** the latter interaction is absent and this destabilizes this structure. The CH ··· O interactions described in these species have been analyzed by Scheiner and co-workers[22] who have categorized them as true H-bonds. The latter claim that the CH ··· O interaction behaves very much like a conventional OH ··· O H-bond in most respects, including shifts in electron density that accompany the formation of the bond and the magnitudes of the various components of the interaction energy. The more favorable interaction energies of **TS1*N*-A** and **TS1*O*-A** compared to **TS1*N*-B** and **TS1*O*-B** also show the importance of CH ··· O interactions in stabilizing these transition states.

The role of Cieplak effects, the $\sigma_{C-X} \rightarrow \sigma_{\ddagger}^*$ and/or $\sigma_{\ddagger} \rightarrow \sigma_{C-X}^*$ hyperconjugative interactions, contributes to the diastereoselectivity of reactions **1**.[23a–23d] The large preference of **TS1*N*-A** (**TS1*O*-A**) over **TS1*N*-B** (**TS1*O*-B**) can also be attributed to the antiperiplanar location of the CH_3 group to the critical bond in the transition states. The preference for the dienophile attack to the diene face bearing the methoxy group is consistent with experimental data from other Diels–Alder reactions.[23e] The influence of Cieplak effects can be clearly inferred from the significant lengthening of the *anti* C–C bond (relative to incipient C ··· C bonds) in the transition structures ($d(H_3C–C)_{anti}$ = 1.543 Å in **TS1*N*-A** as compared to $d(H_3C–C)_{syn}$ = 1.531 Å in **TS1*N*-B**; ($d(H_3C–C)_{anti}$ = 1.543 Å in **TS1*O*-A** as compared to $d(H_3C–C)_{syn}$ = 1.536 Å in **TS1*O*-B**) and allows explanation of the synchronicity variations. In compounds **TS1*N*-A**/**TS1*O*-A** electron donation from the methyl group towards the critical bond in the antiperiplanar position shortens the C–C critical bond as compared to their counterparts **TS1*N*-B**/**TS1*O*-B**. The higher distortion in **B** type transition structures – more asynchronous later transition states – as compared to **A** type transition structures can be attributed mainly to the Cieplak effect. Also note that interaction energies – mainly CH ··· O interactions – play a substantial role in stabilizing the transition structure **TS1*N*-A** (**TS1*O*-A**) as compared to **TS1*N*-B** (**TS1*O*-B**). **A** type transition structures have more favored distortion and interaction energies compared to **B** type.

Reaction of 2 with NMM and MA. In this reaction, in the case of **NMM**, **TS2*N*-A** and **TS2*N*-B** are both stabilized by

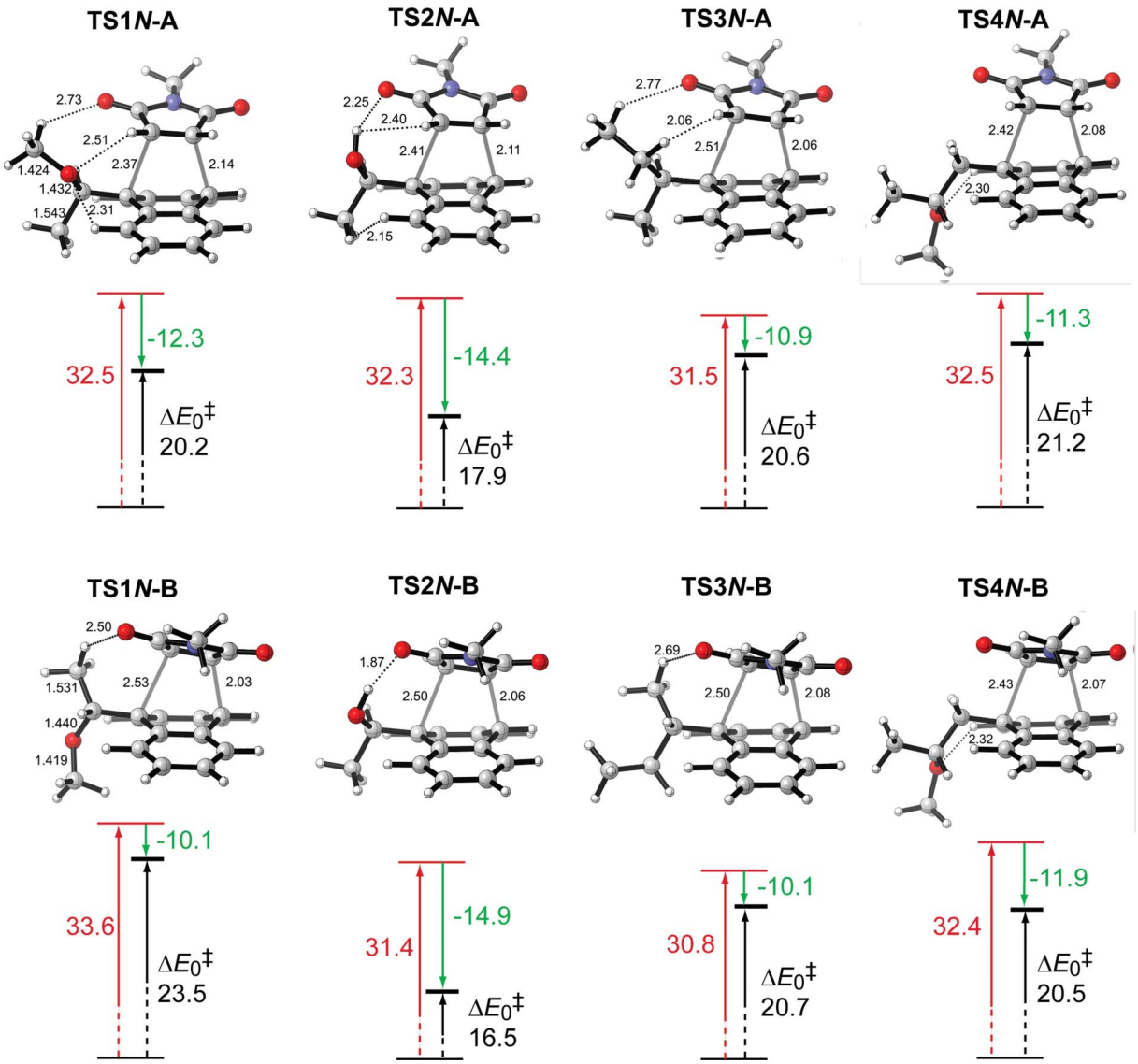

Fig. 1 Transition state geometries, distortion ($\Delta E_{dist}^{\ddagger}$, red), interaction ($\Delta E_{int}^{\ddagger}$, green) and activation energies ($\Delta E_{o}^{\ddagger}$, black) for the cycloadditions of **1–4** with **NMM** (**1*N***, **2*N***, **3*N*** and **4*N***). (B3LYP/6-31+G(d), gas phase).

H-bonding interactions. The O···H distance is shorter in the most stable transition state **TS2*N*-B** (1.87 Å) than it is in **TS2*N*-A** (2.25 Å), however **TS2*N*-A** is more synchronous. In the case of reaction **2** with **MA**, **TS2*O*-B** is stabilized *via* a H-bond between the hydroxyl H (0.546) and the O of **MA** (–0.440) at a distance of 1.92 Å. In **TS2*O*-A**, the H-bond between hydroxyl H (0.510) and the O of **MA** (–0.451) can be considered relatively weaker than in **TS2*O*-B** as can be seen from the larger O···H distance (2.36 Å) and less favorable interaction energy. Despite the stronger H-bonding interaction in **TS2*O*-B** than in **TS2*O*-A**, the latter is sterically favored and also more synchronous. Steric repulsions between the H's of the methyl group with the H's of **MA** in one case and with the H's of anthracene in the other destabilize these structures (Fig. 2).

In the experimental study carried out by Atherton and Jones[5b] the product obtained for reaction **2** was found to be the opposite diastereomer to the one obtained in reaction **1**. The cycloaddition of maleic anhydride occurred with the opposite sense of diastereoselection to that obtained when the Diels–Alder addition reaction is carried out with the *O*-methyl carbinol derivative. The reversal of the diastereoselectivity coupled with the increase in rate observed was explained by considering hydrogen bonding between the alcohol group of the auxiliary and the carbonyl oxygen of maleic anhydride. This was claimed to tether the approach of the dienophile and to override the inherent preference of these systems to undergo cycloaddition with the carbonyl group oriented away from the alkoxy substituent to avoid electrostatic repulsion.

Our results agree with the experimental predictions in both aspects; the presence of H-bonding stabilizes the transition structures of reaction **2** and lowers the barrier as compared to reaction **1**. The interaction energy is substantially larger in **TS2*O*-B** (18.3 kcal mol^{-1}) than in **TS1*O*-A** (16.1 kcal mol^{-1}). Of the 2.5 kcal mol^{-1} difference that favors **TS2*O*-B** over **TS1*O*-A** only 0.3 kcal mol^{-1} arise from the differences in the distortion of the substrates to the transition state geometry. The larger interaction energy (2.2 kcal mol^{-1}) in **TS2*O*-B** as compared to **TS1*O*-A** reflects

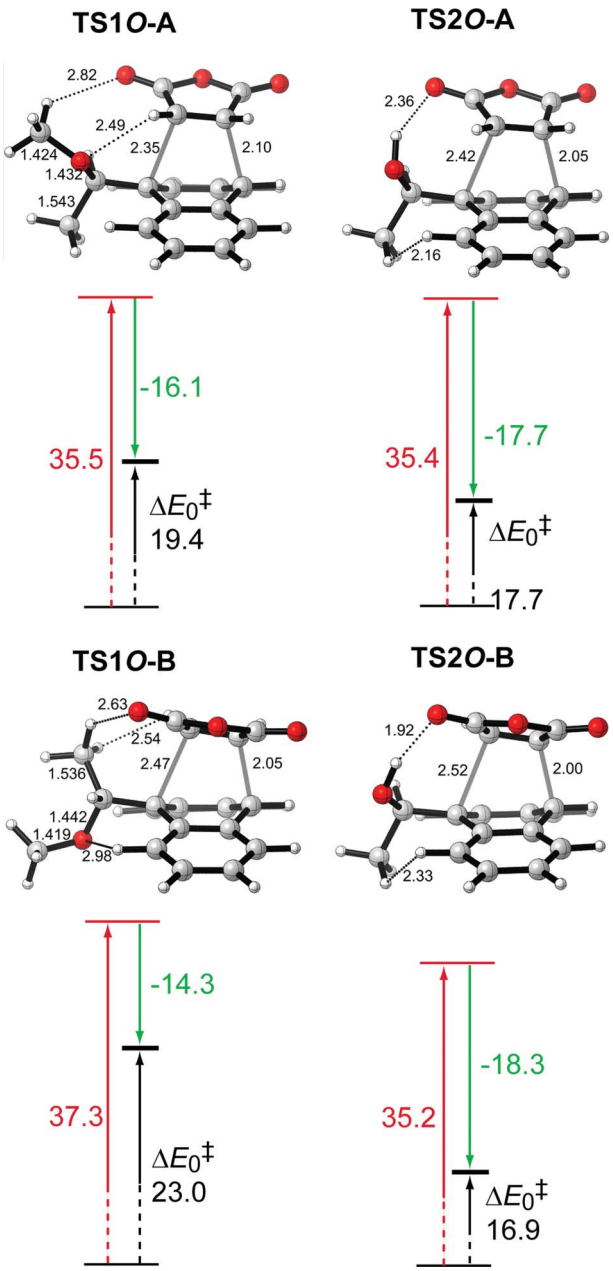

Fig. 2 Transition state geometries, distortion ($\Delta E_{dist}^{\ddagger}$, red), interaction ($\Delta E_{int}^{\ddagger}$, green) and activation energies ($\Delta E_{o}^{\ddagger}$, black) for the cycloadditions of **1** and **2** with **MA** (**1*O*** and **2*O***). (B3LYP/6-31+G(d), gas phase).

the stabilization of the latter by hydrogen bonding. However the identity of the dienophile – **MA**/**NMM** – does not seem to play a major role in the energy barriers even though in the case of **MA** distortion and interaction energies are higher.

Reaction of 3 with NMM. The most stable transition states for reaction **3**, **TS3*N*-A** and **TS3*N*-B** (Fig. 1), are isoenergetic and are stabilized by long range $-CH_2CH_3\cdots O{=}C$ interactions between the methyl group (0.254/0.252) and the carbonyl oxygen (–0.414/–0.419). This reaction is similar to reaction **1**, where the methoxy substituent on the C9 is replaced by an ethyl group. The barriers for the Diels–Alder reaction are slightly higher for reaction **3** than for reaction **1** because the stabilizing methoxy/O–**MA**/H interaction in **TS1*N*-A** is replaced by a repulsive H $\cdots$ H interaction in **TS3*N*-A**. This can also be observed in the less favorable interaction energy of **TS3*N*-A** (–10.9 kcal mol^{-1}) compared to that of **TS1*N*-A** (–12.3 kcal mol^{-1}). Also note that reaction **3** is not as selective as reaction **1** because of the absence of electrostatic interactions stabilizing either one of the transition structures of diastereomers **A** or **B**. Similarly, the distortion and interaction energies in **TS3*N*-A** and **TS3*N*-B** are very close.

Reaction of 4 with NMM. The reaction between compound **4** and **NMM** proceeds *via* **TS4*N*-A** and **TS4*N*-B** to yield diastereomers **A** and **B** (Fig. 1). In these transition states **NMM** approaches the dienophile between the H's from the least crowded part of anthracene. The stereogenic center, even though identical to the one in compound **1**, is placed one carbon away and is not as discriminative between **A** and **B** as in reaction **1*N***. Interaction and distortion energies are quite similar in the case of these two diastereomeric transition structures.

For cycloadditions of **1–4** with **NMM**, the interaction energies ($\Delta E_{int}^{\ddagger}$) are significantly different, while the distortion energies ($\Delta E_{dist}^{\ddagger}$) remain very similar (Fig. 1). The distortion/interaction model shows a linear correlation between the interaction energies of anthracenes **1–4** with **NMM** ($\Delta E_{int}^{\ddagger}$) and the activation energy ($\Delta E_{0}^{\ddagger}$) (Fig. 3, $R^2 = 0.92$, $(\Delta E_{0}^{\ddagger}) = 1.11(\Delta E_{int}^{\ddagger}) + 33.4$). This suggests that the reactivity of anthracenes with different chiral auxiliaries towards a given dienophile is mostly determined by the interaction energy between the diene and the dienophile in the transition state.

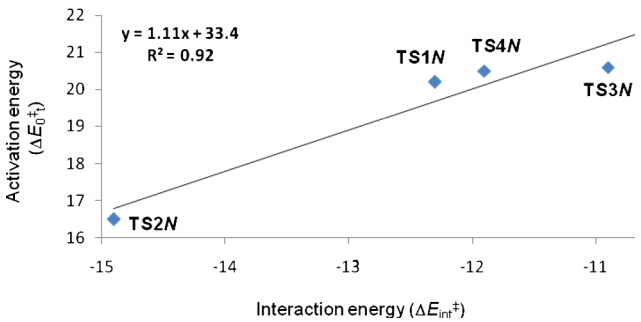

Fig. 3 Correlation between activation energies ($\Delta E_{0}^{\ddagger}$) and interaction energies ($\Delta E_{int}^{\ddagger}$) for the cycloadditions of **1–4** with **NMM** (B3LYP/6-31+G(d)).

The Boltzmann distributions of diastereomers **A** and **B** based on Gibbs free energies of activation have been calculated for reactions **1**, **2**, **3** and **4** (Table S1†). For reaction **1** with **NMM** and **MA** the experimental ratio is quite well reproduced in both media. Similarly for reactions **2**, **3** and **4** the calculated results mimic reasonably well the corresponding experimental findings. **TS1*O*-A**/**TS1*O*-B** as well as **TS2*O*-A**/**TS2*O*-B** have higher dipole moments than the others and their abundance in solution is triggered by the solvent. Note that in the case of reaction **2*O*** the agreement with experimental findings is excellent as the presence of the solvent is taken into account.

2. Stereogenic center and hydrogen bonding effects on the π facial selectivity

One of the key features of the Diels–Alder reaction that generated considerable interest relates to the dramatic changes in the

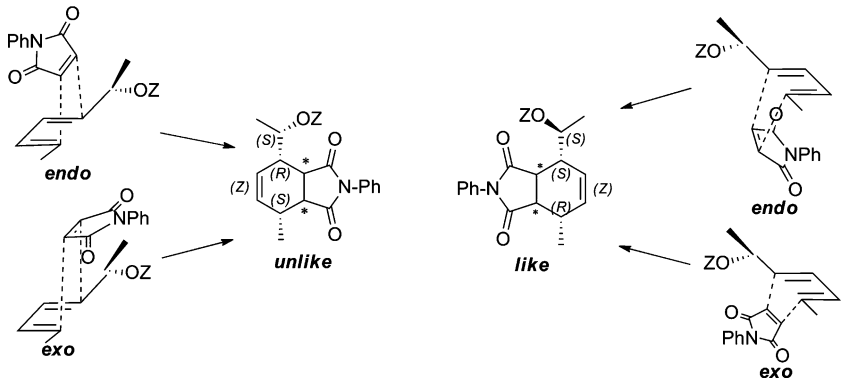

Scheme 2 Diels–Alder Reaction of 1-substituted 1,3-pentadienes with **NPM**. (**5**: Z = CH_3, **6**: Z = H).

product selectivities depending on the nature of the reactants. The ubiquitous example of selectivity in the Diels–Alder reaction when one of the reactants is acyclic is the *endo*/*exo* stereoselectivity observed in [4 + 2] cycloadditions.[24] While the *endo* approach is favored in general, due to the presence of secondary orbital interactions its preference is not unambiguous in all cases.[25] The π-facial selectivity can be induced by linking the diene or the dienophile to a chiral auxiliary.[21] Experimental studies by Tripathy *et al.*[26a] have demonstrated that steric and electronic features of both the diene and the dienophile influence the π-facial selectivity of the Diels–Alder reaction. The term *like* in these reactions describes the dienophile approach on the *re* face of the double bond with an adjacent *R*-configuration allylic center, or *vice versa e.g. si* face with an *S*-configuration center. The reactions with the $(CH_3)(OCH_3)(H)$ and $(CH_3)(OH)(H)$ groups on the stereogenic center of the diene with *N*-phenyl maleimide (**NPM**) as the dienophile are modeled in order to compare the facial selectivity to the selectivity induced by a C9-chiral auxiliary substituted anthracene (Scheme 2). The conformational study of the dienes **5** and **6** has revealed the fact that they both exhibit zigzag-like chain structures (Fig. S1†).

Reaction of 5 and 6 with NPM. The dienophile **NPM** can approach the 1-substituted 1,3-pentadienes from either face – π facial selectivity – and can yield *exo* and *endo* products (Scheme 2). This leads to *like–endo*, *like–exo*, *unlike–endo* and *unlike–exo* transition structures (Fig. 4). Notice that for reaction **5*N*** the transition structures yielding the *endo* products are preferred over the ones that would yield the *exo* products, since the favorable interactions between the methyl group and the oxygen of **NPM** which are present in the former structures are weaker in the latter. The *unlike–endo* structure, **TS5′-*endo***, has the lowest barrier: the dienophile, **NPM** approaches the diene between the hydrogen and the methoxy group. *Unlike–endo*, **TS5′-*endo***, is preferred to *like–endo*, **TS5-*endo***. Both structures are stabilized by CH_3–O interactions; nevertheless in the latter the diene loses its intrinsic stabilizing interactions in order to reach the dienophile. The Boltzmann distribution of **TS5-*endo*** to **TS5′-*endo*** in solution yields qualitative agreement with the experimental one (Table S2†).[26b] The overlap of the secondary orbitals is favored in the *endo* cyclization: in **TS5′-*endo*** the orbital with the lone-pairs on N (**NPM**) overlaps with the orbital of the same sign on the diene, but this stabilizing secondary orbital interaction is lacking in **TS5′-*exo*** (Fig. S5a). The secondary orbital interaction (SOI) model has been widely employed as a conceptually effective framework in explaining the kinetically controlled *endo*-addition in the Diels–Alder reaction.[27] However, this interpretation has also become a subject of considerable controversy.

A combination of effects such as electrostatic, steric, hydrogen bonding, as well as solvent effect can alternatively be invoked to explain the selectivity.[28] The preference for **TS5′-*endo*** (rather than **TS5′-*exo***) can be attributed to the *syn* methoxy approach of **NPM**: this is similar to the *syn* preference in the reactions of a number of 5-substituted cyclopentadienes with several dienophiles.[29] The frontier orbitals in both cases favor the electron flow from the HOMO of the diene to the LUMO of the dienophile: this can be confirmed by the signs of the overlapping orbitals of primary reacting sites (Fig. S5a†); by the $E_{\text{LUMO-NMP}} - E_{\text{HOMO-diene}}$ difference (0.1099) which is favored over the $E_{\text{LUMO-diene}} - E_{\text{HOMO-NMP}}$ difference (0.2121) (Fig. S5b); and by the magnitudes and signs of the HOMO of the diene (**5**) and the LUMO of the dienophile (**NPM**) (Fig. S5c). The same discussion follows for the reaction between **6** and **NPM**: **TS6′-*endo*** is the equivalent of diastereomer **A** where **NPM** approaches the diene between the hydroxyl group and the hydrogen with a H-bonding distance of 1.95 Å (Fig. 4). As in reaction **5** with **NPM**, **TS6′-*endo*** is preferred over **TS6′-*exo*** because the **NPM** ring is distorted at the expense of forming a H-bond in the latter. The Gibbs free energies of activation of the best conformations in "*like*" and "*unlike*" are similar with B3LYP/6-31+G(d): the experimental trend is qualitatively reproduced with BMK/6-31+G(d) in solution. Also note that interaction energies account for the preference of *endo* transition structures (**TS5′-*endo*** and **TS6′-*endo***) as compared to *exo* ones (**TS5′-*exo*** and **TS6′-*exo***) (Table S2†).

3. Kinetics *versus* thermodynamics

Critical distances, asynchronities (Δ*d*, Å), activation barriers ($\Delta E_0^{\ddagger}$), Gibbs free energies of activation ($\Delta G_0^{\ddagger}$), and heats of reaction (ΔH_{rxn}) for reactions **1–6** are summarized in Table 1. All the reactions considered in this study are exothermic: the facilitation due to H-bonding is not reflected in the magnitude of the exothermicities, the reactions are kinetically controlled. The transition states are reactant-like, and the barrier height is obviously not decided by the exothermicity of the overall reaction but rather by the energetics in the early stage of the reaction. The hydrogen bonding effect can be monitored by comparing **TS1*N*-A** with **TS2*N*-B**, **TS1*O*-A** with **TS2*O*B**, **TS5′-*endo*** with

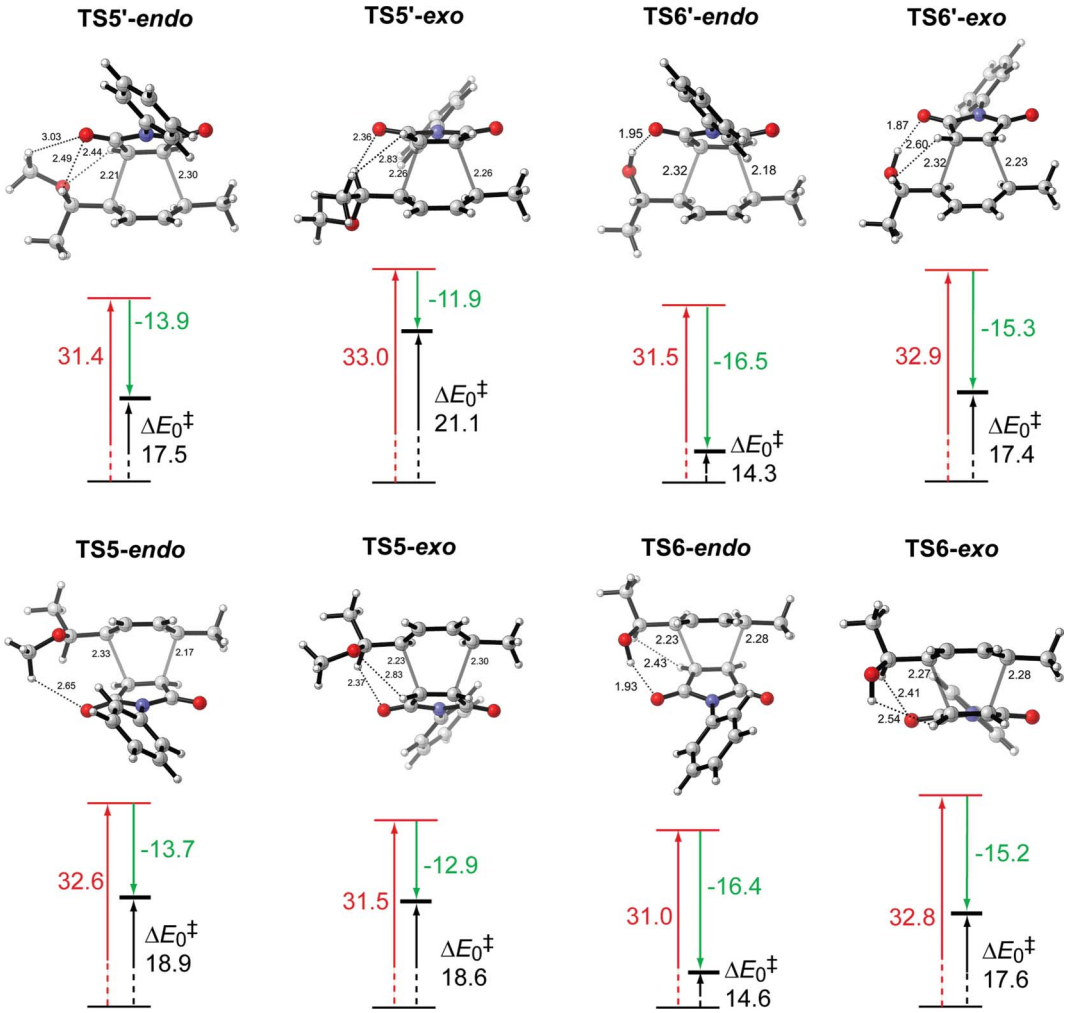

Fig. 4 Transition state geometries, distortion ($\Delta E_{dist}^{\ddagger}$, red), interaction ($\Delta E_{int}^{\ddagger}$, green) and activation energies ($\Delta E_{o}^{\ddagger}$, black) for the cycloadditions of **5** and **6** with **NPM** (B3LYP/6-31+G(d)).

TS6′-*endo*. H-Bonding facilitates the Diels–Alder reaction: for reactions **1*N*/2*N*** the barriers are 20.2/16.5 kcal mol^{-1}, for reactions **1*O*/2*O*** they are 19.4/16.9 kcal mol^{-1} and for reactions **5**–**6** the barrier decreases from 17.5 kcal mol^{-1} to 14.3 kcal mol^{-1}. The transition states that contain a hydrogen bond display a moderate asynchronicity (Δd) as compared to the counterparts that lack this feature. The value of Δd is 0.23 for **1*N*** *versus* 0.44 for **2*N***, 0.25 for **1*O*** *versus* 0.52 for **2*O***, 0.09 for **5** *versus* 0.14 for **6**. Such a situation is consistent with the increase in asynchronicity reported for the butadiene + acrolein reaction when a water molecule is coordinated to the dienophile.[30] **TS3*N*-A** is asynchronous possibly due to the long range stabilizing ($CH_3 \cdots O{=}C$) and destabilizing interactions ($CH_2 \cdots H$) which counterbalance and keep these two parts away from each other. In the case **TS5′-*endo*/TS6′-*endo*** the stabilization by hydrogen bonding amounts to 2.5 kcal mol^{-1}, this is comparable to the difference in Gibbs free energies of activation (Fig. 4 and Table 1). Overall, both in the acyclic system and in anthracene the facilitation due to H-bonding is reflected in the interaction energies. Note that the lower barriers due to H-bonding in the case of reaction **6*N*** are in agreement with the slightly more exothermic character of the latter as compared to **5*N*** (Table 1). Also due to a decrease in steric interactions between the two moieties, the transition structures for **5** and **6** are more synchronous than the ones for reactions **1**–**4**. A reasonable agreement between experimental and calculated diastereomeric percentages has been reproduced with B3LYP/6-31+G(d) (Fig. 5).

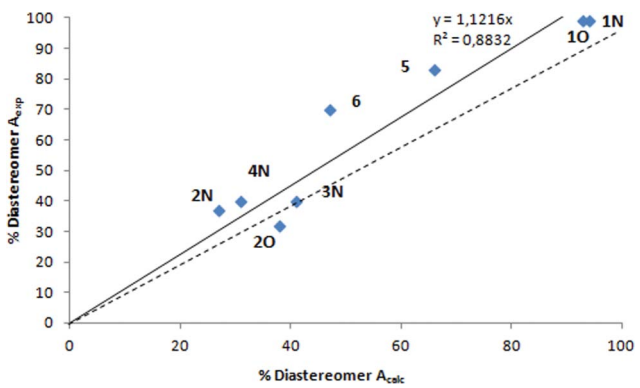

Fig. 5 Correlation between % A_{exp} and % A_{calc} (A = diastereomer adduct in reactions **1**–**6**) (B3LYP/6-31+G(d)).

Table 1 Critical distances, asynchronities (Δd, Å), activation barriers ($\Delta E_0^{\ddagger}$), Gibbs free energies of activation ($\Delta G_0^{\ddagger}$), and heats of reaction (ΔH_{rxn}) for reactions **1–6** (B3LYP/6-31+G(d))

	Critical distances (asynchronicity)	$\Delta E_0^{\ddagger}$	$\Delta G_0^{\ddagger}$	ΔH_{rxn}
TS1*N*-A	2.37 2.14 (0.23)	20.2	38.4	−15.6
TS1*O*-A	2.35 2.10 (0.25)	19.4	37.4	−13.2
TS2*N*-B	2.50 2.06 (0.44)	16.5	36.0	−17.1
TS2*O*-B	2.52 2.00 (0.52)	16.9	35.9	−12.9
TS3*N*-A	2.51 2.06 (0.45)	20.6	39.9	−15.5
TS4*N*-B	2.43 2.07 (0.36)	20.5	38.8	−13.5
TS5-*endo*	2.21 2.30 (0.09)	17.5	32.1	−29.5
TS6-*endo*	2.32 2.18 (0.14)	14.3	29.6	−30.8

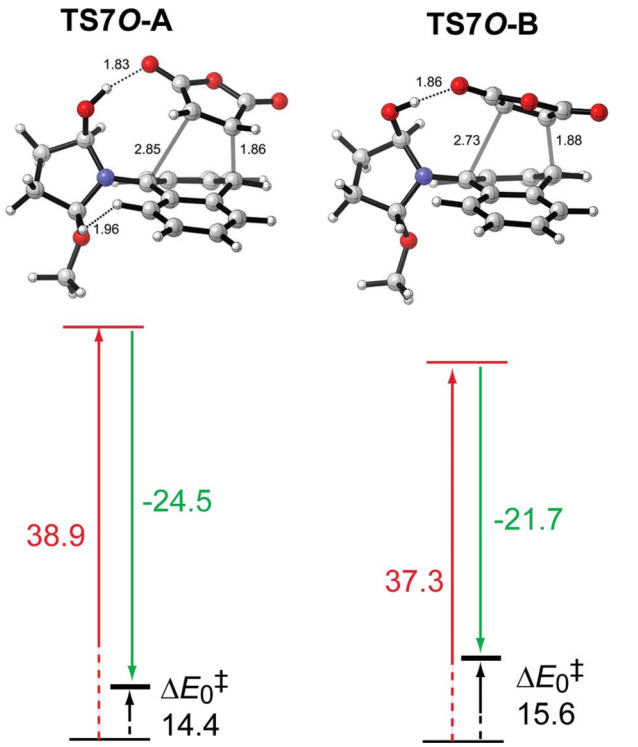

Fig. 6 Transition state geometries, distortion ($\Delta E_{dist}^{\ddagger}$, red), interaction ($\Delta E_{int}^{\ddagger}$, green) and activation energies ($\Delta E_o^{\ddagger}$, black) for the cycloadditions of **7** with **MA**. (B3LYP/6-31+G(d).

4. Can rigid auxiliaries assist the selectivity *via* hydrogen bonding?

Hydrogen bonding due to the presence of the hydroxyl group on the auxiliary increases the reactivity in spite of yielding poor diastereoselectivity as in **TS2*N*** (27 : 73), **TS2*O*** (38 : 62), **TS6** (46 : 54) in benzene. Inspired by the diastereoselectivity study of chiral amino siloxy dienes in the Diels–Alder reaction by Rawal and co-workers,[1] where a rigid five-membered pyrrolidine scaffold is used as an auxiliary, a computational study on (2*R*,5*R*)-1-(anthracen-9-yl)-5-methoxypyrrolidin-2-ol has been carried out. Analysis of **TS7*O*-A** and **TS7*O*-B** (Fig. 6) has revealed the fact that both structures are stabilized by O–H $\cdots$ O bonds of 1.83 Å (α = 161.65°) and 1.86 Å respectively (α = 175.0°). Electron donation from the methyl group of CH_3O to the *anti* C–N bond of the pyrrolidine ring shortens this C–N bond (1.45 Å) as compared to the one in the proximity of the OH group (1.49 Å). The selectivity in this reaction is due to the tilting of the pyrrolidine ring, which is perpendicular to anthracene in the reactant, by 21.1° in **TS7*O*-A** (μ = 7.9 D) in comparison to 33.4° in **TS7*O*-B** (μ = 6.7 D), the former is further stabilized in benzene and the selectivity amounts to 75 : 25 in solution whereas it is 71 : 29 in the gas phase. The selectivity of this reaction is expected to increase in a more polar solvent because of the higher dipole moment of **TS7*O*-A**.

Even though the activation barriers for reaction **7*O*** are lower than the ones for reactions **1–6**, distortion energies are the highest due to the asynchronous nature of **TS7*O*-A** and **TS7*O*-B** (Fig. 6). The interaction energies are also more favorable compared to reactions **1–6**. The stereoselectivity is vastly determined by the more favorable interaction energy of **TS7*O*-A** (−24.5 kcal mol^{-1}) relative to **TS7*O*-B** (−21.7 kcal mol^{-1}), which compensates the slightly higher distortion energy of **TS7*O*-A**.

A plot of interaction energies of the lowest energy transition states for reactions, **1*O***, **2*O*** and **7*O***, *versus* the activation energies shows a linear correlation ($R^2 = 0.93$, $(\Delta E_0^{\ddagger}) = 0.55(\Delta E_{int}^{\ddagger}) + 27.8$). The differences in the slopes of the curves for **NMM** and **MA** (1.11 *vs.* 0.55) suggest that the reactivity of the cycloadditions of anthracenes with **NMM** are more sensitive to changes in the interaction energies compared to their reactions with **MA**.

Conclusions

The nature of the substituents on the stereogenic center plays an important role in the stereoselectivity of the Diels–Alder reaction. The steric and electronic effects induced by the -OCH_3 group on the stereogenic center allow efficient diastereomeric selection, in agreement with Jones' recent claim that **1** can function as an effective chiral auxiliary, allowing efficient recovery and recycling without no loss of enantiomeric excess.[11] In this study the discrimination among the stereoisomers is the best for reaction **1** as well. H-Bonding *via* the OH substituent on the stereogenic center in reaction **2** diminishes the stereospecificity. Modification of –OCH_3 to –OH results in stronger interactions with the dienophile, hence a more facile cycloaddition occurs as can be seen from the decreased activation barriers. The stereogenic center on C9 [-C(H)(OCH_3)(CH_3)] induces a very strong stereoselection; nevertheless this group does not play the same role when attached on a C atom away from C9. The methodology used (B3LYP/6-31+G(d), BMK/6-31+G(d) and M06-2X/6-31+G(d)//B3LYP/6-31+G(d)) to determine the Gibbs activation free energies for every path is incorporated into the Boltzmann distribution to reproduce successfully the

experimental results. The distortion–interaction model shows that the diastereoselectivities and reactivities are mostly governed by interaction energies between the diene and the dienophile. Interaction energy ($\Delta E_{int}^{\ddagger}$) correlates linearly with the activation energy ($\Delta E_{o}^{\ddagger}$). Reactions **5** and **6** with **NPM** yield primarily the *endo* product as expected based on stabilization through H-bonding and secondary orbital-overlap. Note that the barriers for reactions **1** and **2** are higher than the ones for **5** and **6** as anticipated from steric repulsions in the case of anthracene as the substrate. Overall, in Diels–Alder reactions, the nature of the substituents on the stereogenic center and the proximity of the center to the reactive site play a substantial role in diastereoselectivity. The role of hydrogen-bonding should be tackled with care: even though the presence of hydrogen bonding is crucial for reactivity its presence may not increase the diastereoselectivity as in the examples given in this study. We expect that these insights will enable the design of hydrogen-bond assisted/directed cycloadditions that proceed with excellent stereocontrol.

Acknowledgements

Some of the numerical calculations reported in this paper were performed at TUBITAK ULAKBIM, High Performance and Grid Computing Center (TR-Grid e-Infrastructure). Computing resources used in this work were also provided by the National Center for High Performance Computing of Turkey (UYBHM), 20452008. The authors thank the Boğaziçi Üniversitesi Bilimsel Araştırma Projeleri (BAP5156) for financial support.

References

1 (*a*) S. A. Kozmin and V. H. Rawal, *J. Am. Chem. Soc.*, 1999, **121**, 9562–9573 and references therein; (*b*) J. M. Janey, T. Iwama, S. A. Kozmin and V. H. Rawal, *J. Org. Chem.*, 2000, **65**, 9059–9068.
2 (*a*) E. Winterfeldt, *Chem. Rev.*, 1993, **93**, 827–843 and references therein; (*b*) E. Winterfeldt, C. Borm and F. Nerenz, *Adv. Asymm. Syn.*, 1997, **2**, 1–53 and references therein; (*c*) K. Goldenstein, T. Fendert, P. Proksch and E. Winterfeldt, *Tetrahedron*, 2000, **56**, 4173–4185; (*d*) M. Wolter, C. Borm, E. Merten, R. Wartchow and E. Winterfeldt, *Eur. J. Org. Chem.*, 2001, 4051–4060; (*e*) M.-E. Trân-Huu-Dâu, R. Wartchow, E. Winterfeldt and Y.-S. Wong, *Chem.–Eur. J.*, 2001, **7**, 2349–2369; (*f*) C. Knappwost-Gieseke, F. Nerenz, R. Wartchow and E. Winterfeldt, *Chem.–Eur. J.*, 2003, **9**, 3849–3858.
3 A. J. H. Klunder, J. Zhu and B. Zwanenburg, *Chem. Rev.*, 1999, **99**, 1163–1190.
4 (*a*) A. Sanyal and J. K. Snyder, *Org. Lett.*, 2000, **2**, 2527–2530; (*b*) M. S. Corbett, X. Liu, A. Sanyal and J. K. Snyder, *Tetrahedron Lett.*, 2003, **44**, 931–935; (*c*) K. L. Burgess, M. S. Corbett, P. Eugenio, N. J. Lajkiewicz, X. Liu, A. Sanyal, W. Yan, Q. Yuan and J. K. Snyder, *Bioorg. Med. Chem.*, 2005, **13**, 5299–5309; (*d*) A. Sanyal, Q. Yuan and J. K. Snyder, *Tetrahedron Lett.*, 2005, **46**, 2475–2478; (*e*) K. L. Burgess, N. J. Lajkiewicz, A. Sanyal, W. Yan and J. K. Snyder, *Org. Lett.*, 2005, **7**, 31–34; (*f*) A. L. Jones, X. Liu and J. K. Snyder, *Tetrahedron Lett.*, 2010, **51**, 1091–1094.
5 (*a*) S. Jones and J. C. C. Atherton, *Tetrahedron: Asymmetry*, 2001, **12**, 1117–1119; (*b*) J. C. C. Atherton and S. Jones, *Tetrahedron Lett.*, 2001, **42**, 8239–8241; (*c*) J. C. C. Atherton and S. Jones, *Tetrahedron Lett.*, 2002, **43**, 9097–9100; (*d*) J. C. C. Atherton and S. Jones, *J. Chem. Soc., Perkin Trans. 1*, 2002, 2166–2173; (*e*) R. A. Bawa and S. Jones, *Tetrahedron*, 2004, **60**, 2765–2770.
6 N. Çelebi-Ölçüm, A. Sanyal and V. Aviyente, *J. Org. Chem.*, 2009, **74**, 2328–2336.
7 (*a*) S. E. Wheeler, A. J. McNeil, P. Müller, T. M. Swager and K. N. Houk, *J. Am. Chem. Soc.*, 2010, **132**, 3304–3311; (*b*) Y. Lam, P. H. Cheong, J. M. B. Mata, S. J. Stanway, V. Gouverneur and K. N. Houk, *J. Am. Chem. Soc.*, 2009, **131**, 1947–1957; (*c*) G. O. Jones, V. A. Guner and K. N. Houk, *J. Phys. Chem. A*, 2006, **110**, 1216–1224; (*d*) G. Ujaque, J. E. Norton and K. N. Houk, *J. Org. Chem.*, 2002, **67**, 7179–7184; (*e*) X. Zhang, Q. Deng, S. H. Yoo and K. N. Houk, *J. Org. Chem.*, 2002, **67**, 9043–9053; (*f*) A. Heine, E. A. Stura, J. T. Yli-Kauhaluoma, C. Gao, Q. Deng, B. R. Beno, K. N. Houk, K. D. Janda and I. A. Wilson, *Science*, 1998, **279**, 1934–1940; (*g*) J. Xu, Q. Deng, J. Chen, K. N. Houk, J. Bartek, D. Hilvert and I. A. Wilson, *Science*, 1999, **286**, 2345–2348; (*h*) J. B. Siegel, A. Zanghellini, H. M. Lovick, G. Kiss, A. R. Lambert, J. L. St. Clair, J. L. Gallaher, D. Hilvert, M. H. Gelb, B. L. Stoddard, K. N. Houk, F. E. Michael and D. Baker, *Science*, 2010, **329**, 309–313.
8 X. Zhang and T. C. Bruice, *J. Am. Chem. Soc.*, 2007, **129**, 1001–1007.
9 J. I. García, J. A. Mayoral and L. Salvatella, *J. Org. Chem.*, 2005, **70**, 1456–1458.
10 (*a*) D. P. Curran, S.-M. Choi, S. A. Gothe and F.-t. Lin, *J. Org. Chem.*, 1990, **55**, 3710–3712; (*b*) P. Caramella and G. Cellerino, *Tetrahedron Lett.*, 1974, **15**, 229–232; (*c*) P. Caramella, F. M. Albini, D. Vitali, N. G. Rondan, Y.-D. Wu, T. R. Schwartz and K. N. Houk, *Tetrahedron Lett.*, 1984, **25**, 1875–1878; (*d*) M. Burdisso, R. Gandolfi, P. Pevarello and A. Rastelli, *Tetrahedron Lett.*, 1987, **28**, 1225–1228; (*e*) L. Dal Bola, M. De Amici, C. De Micheli, R. Gandolfi and K. N. Houk, *Tetrahedron Lett.*, 1989, **30**, 807–810; (*f*) D. P. Curran and S. A. Gothe, *Tetrahedron*, 1988, **44**, 3945–3952. For leading references on electrophilic addition reactions, see: (*g*) S. D. Kahn, C. F. Pau, A. R. Chamberlin and W. J. Hehre, *J. Am. Chem. Soc.*, 1987, **109**, 650–663 and references therein.
11 H. Adams, T. M. Elsunaki, I. Ojea-Jiménez, S. Jones and A. J. H. M. Meijer, *J. Org. Chem.*, 2010, **75**, 6252–6262.
12 (*a*) D. H. Ess and K. N. Houk, *J. Am. Chem. Soc.*, 2007, **129**, 10646–10647; (*b*) F. Schoenebeck, D. H. Ess, G. O. Jones and K. N. Houk, *J. Am. Chem. Soc.*, 2009, **131**, 8121–8133; (*c*) S Catak, M. D'hooghe, N. De Kimpe, M. Waroquier and V. Van Speybroeck, *J. Org. Chem.*, 2010, **75**, 885–896; (*d*) D. H. Ess and K. N. Houk, *J. Am. Chem. Soc.*, 2008, **130**, 10187–10198; (*e*) G. T. de Jong and F. M. Bickelhaupt, *ChemPhysChem*, 2007, **8**, 1170–1181; (*f*) M. J. van Eis, F. M. Bickelhaupt, S. van Loon, M. Lutz, A. L. Spek, W. H. de Wolf, W. J. van Zeist and F. Bickelhaupt, *Tetrahedron*, 2008, **64**, 11641–11646; (*g*) W. J. van Zeist and F. M. Bickelhaupt, *Org. Biomol. Chem.*, 2010, **8**, 3118–3127.
13 (*a*) L. R. Domingo, M. J. Aurell, M. Arnó and J. A. Sáez, *J. Org. Chem.*, 2007, **72**, 4220–4227; (*b*) A. Padwa, K. R. Crawford, C. S. Straub, S. N. Pieniazek and K. N. Houk, *J. Org. Chem.*, 2006, **71**, 5432–5439; (*c*) S. N. Pieniazek and K. N. Houk, *Angew. Chem., Int. Ed.*, 2006, **45**, 1442–1445.
14 L. R. Domingo, M. T. Picher and J. Andrés, *J. Org. Chem.*, 2000, **65**, 3473–3477.
15 (*a*) A. D. Becke, *J. Chem. Phys.*, 1993, **98**, 1372–1377; (*b*) A. D. Becke, *J. Chem. Phys.*, 1993, **98**, 5648–5652.
16 M. J. Frisch *et al.*, *Gaussian 03, revision D.01*, Gaussian, Inc., Wallingford, CT, 2004.
17 (*a*) C. Gonzalez and H. B. Schlegel, *J. Chem. Phys.*, 1989, **90**, 2154–2161; (*b*) C. Gonzalez and H. B. Schlegel, *J. Phys. Chem.*, 1990, **94**, 5523–5527.
18 M. J. Frisch *et al.*, *Gaussian 09, revision A.1*, Gaussian, Inc., Wallingford, CT, 2009.
19 A. D. Boese and J. M. L. Martin, *J. Chem. Phys.*, 2004, **121**, 3405–3416.
20 Y. Zhao and D. G. Truhlar, *Theor. Chem. Acc.*, 2008, **120**, 215–241.
21 (*a*) B. Mennucci and J. Tomasi, *J. Chem. Phys.*, 1997, **106**, 5151–5158; (*b*) B. Mennucci, E. Cancès and J. Tomasi, *J. Phys. Chem. B*, 1997, **101**, 10506–10517; (*c*) J. D. Thompson, C. J. Cramer and D. G. Truhlar, *J. Chem. Phys.*, 2003, **119**, 1661–1670; (*d*) C. P. Kelly, C. J. Cramer and D. G. Truhlar, *J. Chem. Theory Comput.*, 2005, **1**, 1133.
22 (*a*) Y. Gu, T. Kar and S. Scheiner, *J. Am. Chem. Soc.*, 1999, **121**, 9411–9422; (*b*) T. Kar and S. Scheiner, *J. Phys. Chem. A*, 2004, **108**, 9161–9168.
23 (*a*) A. S. Cieplak, *Chem. Rev.*, 1999, **99**, 1265–1336; (*b*) J. B. Macaulay and A. B. Fallis, *J. Am. Chem. Soc.*, 1990, **112**, 1136–1144; (*c*) J. M. Coxon, R. D. J. Froese, B. Ganguly, A. P. Marchand and K. Morokuma, *Synlett*, 1999, **11**, 1681–1703; (*d*) G. Mehta and R. Uma, *Acc. Chem. Res.*, 2000, **33**, 278–286; (*e*) J. R. Gillard and D. J. Burnell, *J. Chem. Soc., Chem. Commun.*, 1989, 1439–1440.
24 (*a*) R. Hoffmann and R. B. Woodward, *J. Am. Chem. Soc.*, 1965, **87**, 4388–4389; (*b*) M. A. Fox, R. Cardona and N. J. Kiwiet, *J. Org. Chem.*, 1987, **52**, 1469–1474.
25 G. Gayatri and G. N. Sastry, *J. Phys. Chem. A*, 2009, **113**, 12013–12021.
26 (*a*) R. Tripathy, R. W. Franck and K. D. Onan, *J. Am. Chem. Soc.*, 1988, **110**, 3257–3262; (*b*) W. Adam, J. Gläser, K. Peters and M. Prein, *J. Am. Chem. Soc.*, 1995, **117**, 9190–9193.

27 (*a*) L Salem, *J. Am. Chem. Soc.*, 1968, **90**, 553–566; (*b*) P. V. Alston, R. M. Ottenbrite and T. Cohen, *J. Org. Chem.*, 1978, **43**, 1864–1867; (*c*) D. Ginsburg, *Tetrahedron*, 1983, **39**, 2095–2135; (*d*) R. Gleiter and M. C. Böhm, *Pure Appl. Chem.*, 1983, **55**, 237–244; (*e*) D. M. Birney and K. N. Houk, *J. Am. Chem. Soc.*, 1990, **112**, 4127–4133; (*f*) D. A. Singleton, *J. Am. Chem. Soc.*, 1992, **114**, 6563–6564; (*g*) T. Ohwada, *Chem. Rev.*, 1999, **99**, 1337–1375; (*h*) A. Arrieta, F. P. Cossío and B. Lecea, *J. Org. Chem.*, 2001, **66**, 6178–6180; (*i*) C. S. Wannere, A. Paul, R. Herges, K. N. Houk, H. F. Schaefer III and R.v.P. Schleyer, *J. Comput. Chem.*, 2007, **28**, 344–361.
28 (*a*) J. I. García, J. A. Mayoral and L. Salvatella, *Acc. Chem. Res.*, 2000, **33**, 658–664; (*b*) J. I. García, J. A. Mayoral and L. Salvatella, *Eur. J. Org. Chem.*, 2005, 85–90.
29 M. Ishida, T. Aoyama, Y. Beniya, S. Yamabe, S. Kato and S. Inagaki, *Bull. Chem. Soc. Jpn.*, 1993, **66**, 3430–3439.
30 S. Kong and J. D. Evanseck, *J. Am. Chem. Soc.*, 2000, **122**, 10418–10427.

